Correlations and Disorder in Arrays of Magnetically Coupled Superconducting Rings

Dragomir Davidović,[1] Suman Kumar,[1] Daniel H. Reich,[1]
Jeffrey Siegel,[2] S. B. Field,[2] R. C. Tiberio,[3] R. Hey,[4] K. Ploog[4]
[1]*Department of Physics and Astronomy, The Johns Hopkins University, Baltimore, Maryland 21218*
[2]*Department of Physics, University of Michigan, Ann Arbor, Michigan 48109*
[3]*Cornell Nanofabrication Facility, Cornell University, Ithaca, New York 14853*
[4]*Paul-Drude-Institut für Festkörperelektronik, D-10117 Berlin, Germany*
(Received 17 August 1995)

We have used ultrasensitive susceptibility techniques and scanning Hall probe microscopy to study arrays of electrically isolated micron-sized superconducting rings. The magnetic moments produced by the supercurrents in these rings are analogous to Ising spins, and neighboring rings interact antiferromagnetically via their dipolar magnetic fields. We find that there are significant antiferromagnetic correlations between rings, and effects due to geometrical frustration can be observed. Quenched disorder also plays a significant role, suppressing the development of true long-range order.

PACS numbers: 74.25.Ha, 05.50.+q, 74.55.+h, 75.50.Ee

The magnetic properties of an isolated superconducting ring are well understood. As an external magnetic field is ramped up from zero, a circulating current develops in the ring to satisfy the requirement that the superconducting order parameter be single valued. However, as the magnetic flux threading the ring passes $\Phi_0/2 = (hc/2e)/2$ (or any half-integral fraction of Φ_0), it becomes energetically favorable for the current to abruptly change its direction, and then decrease towards zero as the flux is further increased [1]. Exactly at $\Phi_0/2$, the two current directions are energetically degenerate, and are analogous to the two possible orientations of an Ising spin. Now consider two such rings placed in close proximity. Suppose the flux through the first ring is slightly *greater* than $\Phi_0/2$. This will break the degeneracy and cause a current to circulate in the ring which produces a magnetic dipole moment parallel to the applied field. Using the Ising analogy, we call this orientation "spin up." The first ring's dipole field will then point down at the position of the second ring. The flux through that ring will thus be somewhat *less* than $\Phi_0/2$, and its current will circulate in the opposite sense to that in the first ring, leading to a "down spin." The dipole field from the second ring in turn stabilizes the first ring in the spin-up state. A similarly stable state occurs if the first ring is in the down state and the second is in the up state. Thus two closely spaced rings near $\Phi_0/2$ have an *antiferromagnetic* (AFM) coupling. In this paper we present the first experimental results on the magnetic properties of arrays of closely spaced micron-sized superconducting rings.

Low-dimensional antiferromagnets are an area of much current interest in the field of magnetism, and there are important unanswered questions about the effects of lattice geometry, competing interactions, and disorder on the ordering and dynamic properties of such systems [2]. By making our spin systems lithographically we have considerable freedom to tailor their properties, permitting direct experimental comparison of bipartite systems such as the square and honeycomb lattices, which can support Néel order, with geometrically frustrated ones such as the triangular and kagomé lattices, which cannot. We have studied lattices of these four types using a combination of SQUID magnetometry and scanning Hall probe microscopy. We find that there are significant antiferromagnetic correlations in the arrays, and effects due to lattice geometry can be observed. However, because the magnetic coupling between rings is weak, disorder limits the development of long-range correlations.

Arrays containing between 1.6×10^5 and 2.4×10^5 aluminum rings (inset, Fig. 1) were made on sapphire substrates at the Cornell Nanofabrication Facility (CNF) by electron beam lithography and liftoff. Typical array dimensions were 800 μm $\times$ 800 μm. The rings had linewidths of 0.4 μm, and thicknesses of 0.23 μm. The square lattice arrays were composed of square rings with

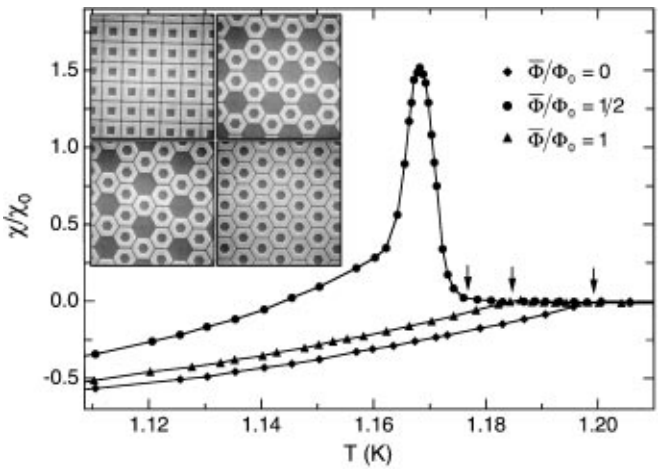

FIG. 1. ac susceptibility χ vs T for a dense square lattice of Al rings. The peak has a FWHM of 5.5 mK. The arrows denote the critical temperatures T_c for (left to right) $\overline{\Phi} = \Phi_0/2$, $\overline{\Phi} = \Phi_0$, and $\overline{\Phi} = 0$. The inset shows SEM micrographs of (clockwise from upper left) square, honeycomb, triangular, and kagomé lattices of rings. Ring dimensions are given in the text.

outside dimension 1.6 μm, and center-to-center distance 1.8 μm. The triangular, honeycomb, and kagomé lattice arrays were composed of hexagonal rings with outside side-to-side dimension 1.73 μm and center-to-center spacing 1.93 μm. Sparse arrays of square rings, with center-to-center distances of 4.0 μm, were made to test the effect of varying the inter-ring coupling strength, which is proportional to M, the mutual inductance between rings. For near neighbors, we calculate $M = 67$ fH for the dense arrays and $M = 4$ fH for the sparse arrays.

The ac susceptibility $\chi(H,T)$ of the arrays was measured as a function of dc field H and temperature T with a SQUID magnetometer mounted on a dilution refrigerator. With $H_{ac} = 6$ mG rms at frequency $f = 3$ Hz, the ac response was linear for all H and T, and the total ac moment produced by the arrays was $\approx 1 \times 10^{-9}$ emu for $T \ll T_c$.

Figure 1 shows the temperature dependence of the ac susceptibility $\chi(T)$ for a dense square array at thre fields $H = 0$, 7.50, and 15.0 G, corresponding to an average applied flux $\overline{\Phi} = 0$, $\Phi_0/2$, and Φ_0 per ring. χ is shown normalized to χ_0, the low-temperature limiting value at $H = 0$. At $\overline{\Phi} = 0$ and $\overline{\Phi} = \Phi_0$, one finds a diamagnetic response due to both the Meissner effect in the body of the rings and the development of flux quantization at low temperatures. For $\overline{\Phi} = \Phi_0/2$, T_c is suppressed due to the Little-Parks effect [3]. $T_c(\Phi_0)$ is less than $T_c(0)$ due to the finite width of the rings [4]. At $\overline{\Phi} = \Phi_0/2$, as T is lowered below $T_c = 1.176$ K, the susceptibility begins to rise dramatically. This paramagnetic response is analogous to the ac susceptibility of a spin system, because for $T \simeq T_c$ thermal fluctuations [5] allow the rings to flip between their spin-down and spin-up states in response to the ac field. One important difference between a ring and a true spin, however, is that for a ring the paramagnetic rise is much faster than $1/T$ because the ring's moment μ increases as $\mu \propto 1 - T/T_c$ [6]. As T is further reduced the paramagnetic response peaks at $T_P = 1.168$ K, and then drops rapidly. This rapid drop arises because the energy barrier between the up and down states grows rapidly with falling temperature [5]. When the thermally activated flipping rate drops below f, the ac response is suppressed. The residual paramagnetic response below the peak and subsequent crossover to diamagnetic behavior arise because after the rings are frozen, χ reflects the slope of the $M(H)$ curve for the up or down state [7]. All of the arrays had $\chi(T)$ very similar to the curves shown in Fig. 1.

We have also measured the field dependence of χ at fixed temperature near T_P. These measurements illustrate two crucial features of our system. First, there is disorder in the arrays that plays the role of a random field in an Ising system. Second, there are AFM interactions between the rings. Figure 2 shows $\chi(\overline{\Phi})$ both above and below T_P for the sparse [Figs. 2(a), 2(c)] and dense [Figs. 2(b), 2(d)] square lattices. At each temperature the field was swept up (open symbols) and down (filled symbols). Each sweep shows a sharp peak in a narrow range spanning $\overline{\Phi} = \Phi_0/2$. The width of this peak shows that there is a distribution of fields $H_{1/2}$ needed to produce $\Phi_0/2$ in the individual rings. Only those rings for which H equals $H_{1/2}$ can flip between the up and down states and contribute strongly to χ. This spread in $H_{1/2}$ arises from variations in the effective areas A enclosed by the rings, and hence the spread in A provides an effective random magnetic field at each site. $\chi(H)$ at each T is fit very well by a Gaussian peak superimposed on a sloping background, as shown by the solid lines in Fig. 2. This background is the response of the nonflipping rings discussed above. Because of the rings' finite width, up and down rings have different current distributions, and hence different susceptibilities, leading to the field dependence of the background.

For the dense array only, as T is reduced the peak in $\chi(H)$ occurs at a lower field for increasing than for decreasing H. This splitting is a signature of the AFM interaction between rings. At the start of the increasing field sweep, $H < H_{1/2}$ for all the rings, and they all are in the down state. Each ring feels the net dipole field H_d of its neighbors, however, which is in the same direction as H. This means that a smaller value of H is needed to reach $H_{1/2}$ for each ring than for the noninteracting case, and the peak in $\chi(H)$ shifts to lower field. The reverse is true when sweeping H down from above. We also note that if the size of the splitting reflects H_d, it should be proportional to the lattice coordination number z. Indeed, the ratio between the splittings for the triangular ($z = 6$) and honeycomb ($z = 3$) lattices is 2.2.

Susceptibility measurements demonstrate the presence of magnetic interactions in the arrays, but provide no evidence for ordering. To address this, we used a scanning Hall probe microscope (SHM) [8] to image specific magnetic configurations of the arrays. The GaAs/AlGaAs Hall probes had active areas of 1 μm^2, and a sensitivity of about $5\text{mG}/\sqrt{\text{Hz}}$. The SHM was mounted on a closed cycle ^{3}He cryostat, and the probe was scanned over the sample

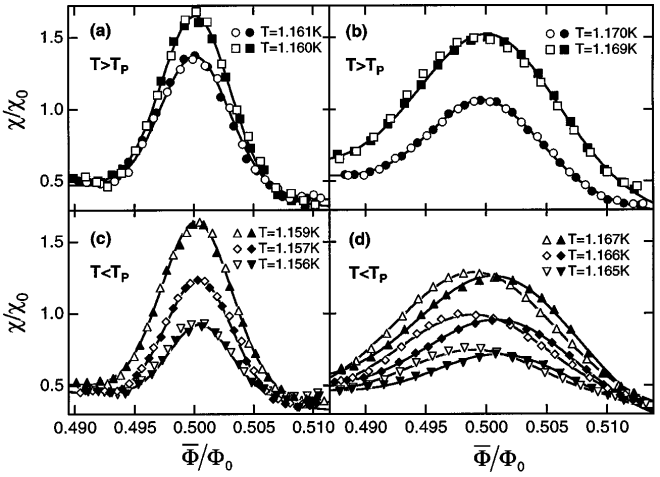

FIG. 2. ac susceptibility χ vs $\overline{\Phi}$ for sparse (a), (c), and dense (b), (d) square lattices of superconducting rings. Open (solid) symbols are for increasing (decreasing) dc field. The splitting in the dense array at lower temperatures reflects inter-ring interactions. The solid lines are Gaussian fits described in the text.

in a noncontact mode at a height of 0.5 μm above the top surface of the rings.

The magnetic field distribution above the arrays was imaged by field cooling from above T_c to $T \approx 0.6T_c$, where the shielding currents in the rings have built up enough to be measured by the Hall probe. We note, however, that the ring *dynamics* begin to freeze out only some 7 mK below T_c (i.e., below the peak of Fig. 1). Thus, these images reflect the spin configurations frozen in near T_P, where the shielding is weak and the flux through each ring is very nearly the applied flux. The arrays were typically cooled through T_c at a rate of 30–50 mK/s, but essentially identical results were obtained at cooling rates as low as 17 μK/s.

Figure 3 shows gray-scale images taken at $T = 0.66$ K of the magnetic field modulation produced by a honeycomb array in five different fields near $\Phi_0/2$. These images cover an area 50×60 μm^2 containing approximately 680 rings near the center of the array. The full-scale magnetic field modulation in these images is 0.53 G. These pictures illustrate the progression with increasing field of the distribution of flux quanta in the array. At $\overline{\Phi}/\Phi_0 = 0.494$, the great majority of the rings are in the down state. The flux penetrates the array mainly through the holes (i.e., the positions of the missing rings) of the honeycomb lattice, which appear as a faint triangular lattice of circular gray spots. A few rings are in the up state, and these appear as bright spots. As the arrays are cooled in progressively larger fields, more and more rings go into the up state. By $\overline{\Phi}/\Phi_0 = 0.506$ nearly all of the rings are up, the holes appear darker than their surroundings, and the remaining down rings appear as dark spots.

To determine the magnetic configuration of the rings, we first locate the position of each ring in these images. The magnetic field profile of each ring was found empirically to be well fit by a Gaussian. Thus we make an initial guess at the correct spin configuration, and construct the corresponding synthetic image by the superposition of Gaussians of the appropriate sign at each site. Any errors in the spin configuration show up very clearly in the *difference* between this synthetic image and the actual image. In the rightmost image in Fig. 3, we show the synthetic image that models the data at $\overline{\Phi}/\Phi_0 = 0.500$. Below it is the difference image formed by subtracting the model from the data. To demonstrate the effectiveness of our modeling procedure, one spin was deliberately flipped in the synthetic image. This error shows up very clearly in the difference image.

The spin configuration of each image determined in this manner is shown in the lower half of Fig. 3. White hexagons indicate up spins and black hexagons indicate down spins. While the spin configurations are obviously disordered, they are *not* random; there are short-range antiferromagnetic correlations. A useful measure of short-range correlations in disordered systems is the bond order parameter [9] $\sigma = 1 - n_{\mathrm{AF}}/2x_+x_-$, where n_{AF} is the fraction of bonds that are antiferromagnetic, and x_+ and x_- are the concentrations of up and down spins, respectively. σ is proportional to the near-neighbor correlation function and ranges from $+1$ for a ferromagnet, through 0 for a completely random arrangement of spins, to -1 for a Néel state at $x_+ = 0.5$. When $\sigma < 0$, it gives the additional fraction of antiferromagnetic bonds as compared to a completely random configuration.

The open and solid circles in Fig. 4(a) show σ vs x_+ spanning $\overline{\Phi}/\Phi_0 = 1/2$, for two series of images taken in different parts of the array. These data show a distinct dip in the order parameter as x_+ increases from zero. At x_+ close to 0.5, σ attains its maximally negative value of -0.18 ± 0.03. We estimate this error from the purely statistical fluctuation in σ for 680 randomly oriented spins. The fact that σ is less than zero for the entire range of x_+ proves that there are short-range antiferromagnetic correlations between rings. The next-nearest-neighbor correlations, however, were consistent with zero.

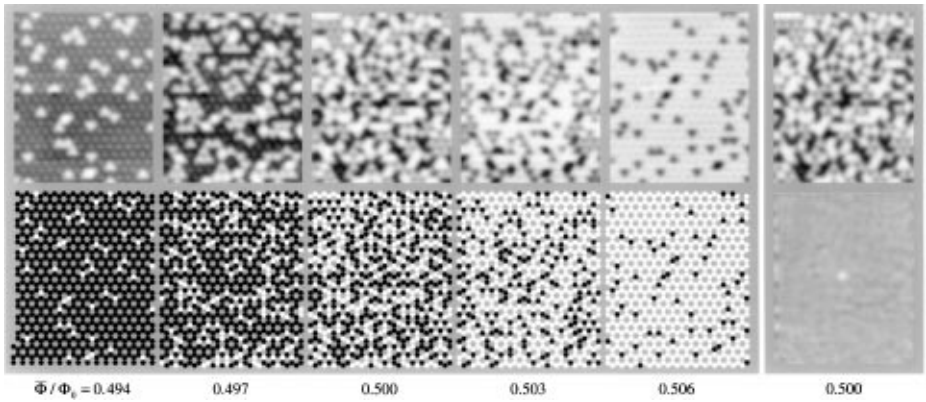

FIG. 3. Top row: The magnetic field above the arrays as imaged by the scanning Hall probe microscope. "Up" spins appear here as white spots, and "down" spins as black ones. The fainter circular spots seen at low spin densities are the positions of the empty spaces of the honeycomb lattice. Bottom row: the spin configurations as deduced from the images. Here, white hexagons represent up spins, and black hexagons down ones. Gray hexagons represent the holes of the lattice. The rightmost frames of the figure are the synthetic image (top) generated from the spin configuration deduced from the $\overline{\Phi}/\Phi_0 = 0.500$ image, and the *difference* (bottom) between the real and synthetic images, when one spin is intentionally flipped.

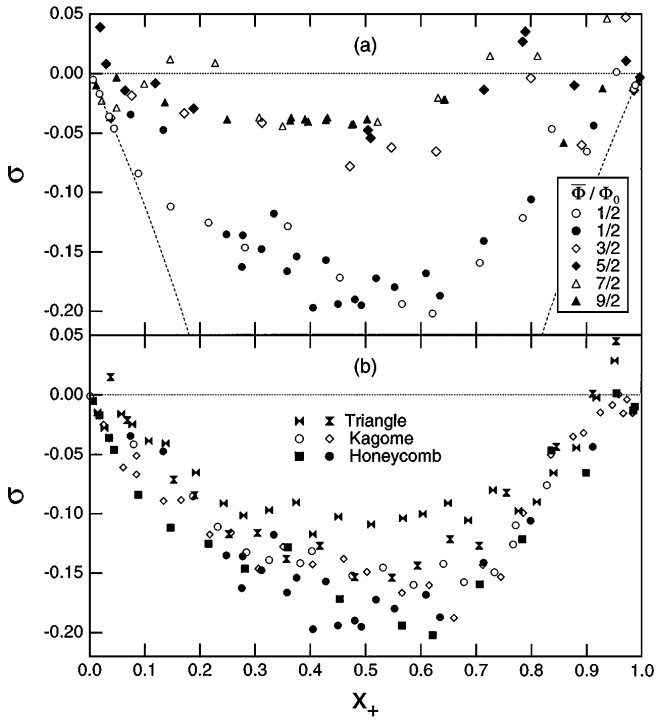

FIG. 4. (a) The bond order parameter σ vs concentration of up spins x_+ for the honeycomb lattice for $\overline{\Phi}/\Phi_0 = 1/2$, $3/2$, $5/2$, $7/2$, and $9/2$. The open and filled circles at $1/2$ were measured at different places in the array. The sloped dashed lines represent the theoretical minimum possible value of σ. (b) The bond order parameter σ vs concentration of up spins x_+ at $\overline{\Phi}/\Phi_0 = 0.5$ for the honeycomb, triangular, and kagomé lattice arrays.

Using the SHM, we also explored the spin configurations at the higher fractions $\overline{\Phi}/\Phi_0 = 3/2, 5/2, 7/2$, and $9/2$. We find (not shown) that the concentration $x + (\overline{\Phi})$ spanning each fraction is well described by an error function, i.e., by an integral of a Gaussian, which again reflects the distribution of flipping fields. The widths of these curves, or equivalently the effective disorder, grows essentially linearly with fraction. This result is expected since the randomness in the flux through the rings, $\Delta\Phi$, equals $H\Delta A$ and so is proportional to H. Thus the disorder in our system is a *tunable* parameter. σ vs x_+ for the honeycomb lattice at the higher fractions is also shown in Fig. 4(a) for the same region of the array as the $\overline{\Phi} \sim \Phi_0/2$ scan shown by solid circles. The order parameter is clearly suppressed from its value at $\Phi_0/2$. This is due to the increased effective disorder at higher fields. However, we see that at higher fractions σ appears to saturate at a nonzero value, which is surprising in view of the increasing disorder. We suggest this is because the interaction strength J grows with field H, keeping the ratio of J to disorder roughly constant. As H is increased, $T_c(H)$ falls [4], so that the coherence length $\xi \sim [T_c(0) - T_c(H)]^{-1/2}$ falls as well. The barrier Δ for flipping, which grows from zero as T is reduced below $T_c(H)$, has a prefactor proportional to ξ, and so will be *less* at higher fields. We expect the spins to freeze into their low-temperature configuration when $\Delta \sim k_B T_c$, which implies the freeze-out temperature T_f is further below $T_c(H)$ at larger H. This gives the current in the rings a greater chance to grow before the rings freeze out. The result [10] is that J grows linearly with field for large H, while at small H, J saturates.

To assess the effects of lattice geometry and frustration, Fig. 4(b) shows σ vs x_+ at $\Phi/\Phi_0 = 1/2$ for honeycomb, kagomé, and triangular lattice arrays. Despite the scatter in the data, it appears that the AFM correlations are stronger in the honeycomb lattice than in the other lattices in the central range around $x_+ = 0.5$, where frustration effects become important. Thus we have direct experimental evidence for geometrical frustration in 2D Ising antiferromagnets.

We have shown that an array of magnetically coupled superconducting rings form a novel realization of an Ising antiferromagnet. There are measurable interactions between rings that lead to hysteretic behavior in $\chi(H)$, and to a finite value of the short-range order parameter σ. We also emphasize that our arrays exhibit very different physics from apparently similar systems such as superconducting wire networks and arrays of Josephson junctions where the coupling between sites is directly through the phase of the superconducting wave function, instead of the magnetic coupling present in our arrays.

We thank M. Höricke for technical assistance with MBE growth, and L. P. Lévy and M. Robbins for stimulating discussions. This work was supported by NSF Grants No. DMR-92-22541 and No. DMR-93-57518, and was performed in part at the Cornell Nanofabrication Facility which is supported by the NSF under Grant No. ECS-8619049, Cornell University and industrial affiliates. D. H. R. acknowledges the support of the David and Lucile Packard Foundation.

[1] M. Tinkham, *Introduction to Superconductivity* (McGraw-Hill, New York, 1975), p. 123.
[2] R. Liebmann, *Statistical Mechanics of Periodic Frustrated Ising Systems* (Springer-Verlag, Berlin, 1986); D. Fisher, G. Grinstein, and A. Khurana, Phys. Today **41**, 56 (1988); T. Nattermann and P. Rujan, Int. J. Mod. Phys. B **3**, 1597 (1989), and references therein.
[3] W. A. Little and R. D. Parks, Phys. Rev. Lett. **9**, 9 (1962).
[4] R. P. Groff and R. D. Parks, Phys. Rev. **176**, 567 (1968).
[5] W. Skocpol and M. Tinkham, Rep. Prog. Phys. **38**, 1049 (1975).
[6] M. Tinkham, *Introduction to Superconductivity*, Ref. [1], Eqs. 4-12 and 4-14.
[7] M is proportional to the current density J, whose H and T dependence for a thin ring near T_c may be found from Eqs. 4-35 and 4-46 in M. Tinkham, *Introduction to Superconductivity*, Ref. [1].
[8] H. D. Hallen *et al.*, Phys. Rev. Lett. **71**, 3007 (1993); A. M. Chang *et al.*, Appl. Phys. Lett. **61**, 1974 (1992); J. Siegel, J. Witt, N. Venturi, and S. B. Field *et al.*, Rev. Sci. Instrum. **66**, 2520 (1995).
[9] J. M. Cowley, Phys. Rev. **77**, 669 (1950).
[10] D. Davidović *et al.* (to be published).